Available online at www.sciencedirect.com
ScienceDirect
Chinese Journal of Aeronautics 20(2007) 193-201
Chinese Journal of Aeronautics
www.elsevier.com/locate/cja

Jet Vectoring Control Using a Novel Synthetic Jet Actuator

LUO Zhen-bing*, XIA Zhi-xun, XIE Yong-gao

College of Aerospace and Materials Engineering, National University of Defense Technology, Changsha 410073, China

Received 8 May 2006; accepted 30 January 2007

Abstract

A primary air jet vectoring control system with a novel synthetic jet actuator (SJA) is presented and simulated numerically. The results show that, in comparison with an existing traditional synthetic jet actuator, which is able to perform the duty of either "push" or "pull", one novel synthetic jet actuator can fulfill both "push" and "pull" functions to vector the primary jet by shifting a slide block inside it. Therefore, because the new actuator possesses greater efficiency, it has potentiality to replace the existing one in various applications, such as thrust vectoring and the reduction of thermal signature. Moreover, as the novel actuator can fulfill those functions that the existing one can not, it may well be expected to popularize it into more flow control systems.

Keywords: jet; vectoring control; synthetic jet actuator; slide block; flow control

The technique of jet vectoring using synthetic jet actuator (SJA) has found wide applications in a number of fields including thrust vectoring, the reduction of thermal signature, gust alleviation, and control surface augmentation or replacement without moving parts[1-4]. Smith and Glezer investigated the jet vectoring by means of SJAs with an "even" exit for the first time[5], and the results showed that jet vectoring with synthetic jets held a bright future. Further, they suggested an actuator with one-sided step exit[6], which performed more effective vectoring function than an actuator with an "even" exit for a given synthetic jet strength and primary jet speed. Afterwards, Guo and Cary simulated the vectoring control of a primary jet by a slope-exit synthetic jet at two angles (0° and 60°)[7]. which showed that the synthetic jet could produce a much larger vectoring angle and vectoring force for the primary jet at 60° than that at 0°. In an actuator with slope-step exit for jet vectoring introduced by the authors[8], the largest vectoring angle was obtained by making use of the actuator with slope-step exit for a given primary jet speed and synthetic jet strength. All of the above studies showed that one existing synthetic jet actuator could perform only one function of either "pull" or "push" in vectoring a primary jet. With the "pull" mode, the synthetic jet is nominally parallel to the primary jet; while in the "push" mode, the synthetic jet impinges normal to the primary jet.

Recently, a new generation of synthetic jet actuators for active flow control is provided[9-10]. Fig.1 shows a schematic diagram of the novel synthetic jet actuator together with a photograph thereof. It consists of two sealed cavities separated on one end by one piezoelectric (PZT) diaphragm, two emitting slots and one slide block (SB). In the novel SJA, the slide block is located in the middle of the two emitting slots; two fluid puffs out of phase are forced out of the actuator in one period of the PZT-diaphragm's vibration, instead of one fluid puff in an existing one. Moreover, the slide block regulates the two

*Corresponding author. Tel.: +86-731-4573099.
E-mail address: luozhenbing@163.com
Foundation item: National Natural Science Foundation of China (90205016, 50176055)

puff jets, thus making the novel synthetic jet actuator possessive of a unique thrust-vectoring characteristic that the existing one does not have [10-11].

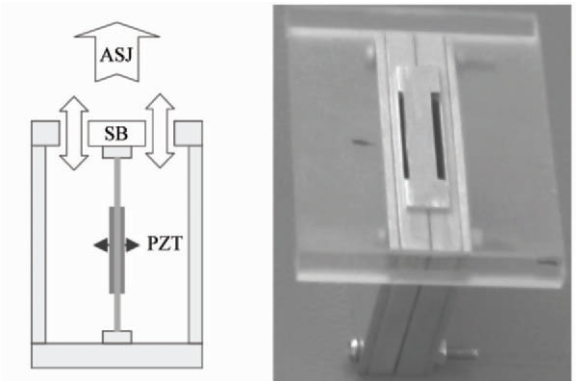

Fig.1 A schematic diagram with a photograph of a novel SJA. SB—slide block; ASJ—adjustable synthetic jet.

The objective of this study is to introduce this novel SJA which has such a unique thrust-vectoring characteristic that it is capable of performing both functions of "push" and "pull" to vector a primary jet.

1 Computation Scheme

1.1 Physical model of jet vectoring control

A schematic diagram of vectoring a primary jet with a novel SJA is shown in Fig.2 which demonstrates the detailed configuration near the exits. The width of the primary jet conduit is H = 20 mm. Parallel to the primary jet, the synthetic jet distances itself from the priamry jet by D = 4 mm, The gap between two exits of the novel SJA i.e. width of the slide block is fixed to be d = 2 mm; the widths of the two exit slots, h_1 and h_2, are equal to 1 mm in the baseline cases.

1.2 Computational method

In this paper, an incompressible flow solver, INS2D, is used for the simulation at very low Mach numbers. The incompressible code has an advantage over the compressible in operation efficiency because the former requires tiny time intervals to achieve stability when running at very low Mach numbers. Accordingly, the unsteady and incompressible Reynolds-averaged Navier-Stokes (RANS) equations are solved. Based on the principle of the conservation of mass and momentum, the incompressible governing equations are derived from the continuity equation and the Navier-Stokes equations,

$$\nabla \cdot \bar{\boldsymbol{u}} = \boldsymbol{0}$$
$$\rho \frac{\partial \bar{\boldsymbol{u}}}{\partial t} + \rho \bar{\boldsymbol{u}} \cdot \nabla \bar{\boldsymbol{u}} = -\nabla \bar{\boldsymbol{p}} + \left(\mu_{\mathrm{l}} + \mu_{\mathrm{t}}\right) \nabla^2 \bar{\boldsymbol{u}} \tag{1}$$

where the over-bar represents a Reynolds-averaged quantity, μ_{l} and μ_{t} denote molecular viscosity and turbulent viscosity, respectively.

The RNG-based k-ε turbulence model is derived from the instantaneous Navier-Stokes equations by a mathematical technique called "renormalization group" (RNG) method. The RNG model is more sensible to the effects of rapid strain and streamlines curvature than the standard k-ε model, which is credited to the superior performance of the

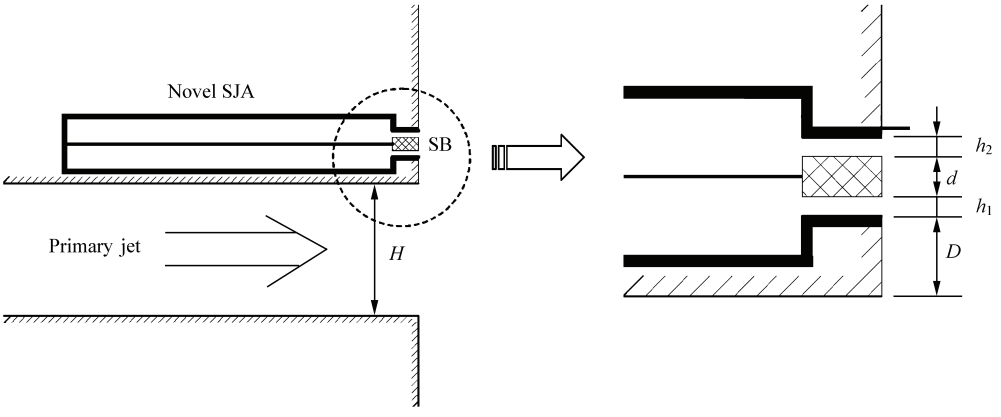

Fig.2 A schematic diagram of a primary jet vectoring control with a novel SJA showing a detailed configuration near the exits.

RNG model for some classes of flows. The enhanced wall treatment is adopted on the base of the two-layer model, in which the whole domain is subdivided into two regions: a viscosity affected region and a fully turbulent one. An upwind differencing scheme based on flux difference splitting is used to compute the convective terms. The second-order is used in the results reported here. The equations are solved by means of a generalized minimum residual scheme with the minimum residual being 1×10^{-4}. The time interval is $T/100$ and sub-iterations amount to 50.

In this study, X-L model[12-14], a computational one for SJA, is adopted, in which the actuator cavity and the exit throat are regarded as a single computational domain. The actuator diaphragm functions electrically with f being a forcing frequency, A_m the amplitude of the vibrating metal diaphragm, r the radius of the metal diaphragm, and φ_0 the original phase of the actuator diaphragm. For an arbitrary point on the diaphragm (y, l), where l is the distance from the point to the center of the diaphragm, the velocity of this point is composed of an axial velocity u_y (l, t) and a radial velocity u_l (l, t). Provided the diaphragm vibrates in cosine form, the functions are given as follows

$$\begin{aligned} u_y(l,t) &= 2\pi f A_m \cdot \left(1-\frac{l^2}{r^2}\right)\cdot \sin(2\pi f t+\varphi_0) \\ u_l(l,t) &\approx 0 \end{aligned} \tag{2}$$

where f = 500 Hz, A_m= 0.2 μm, r = 23 mm, and $\varphi_0 = 0$. The frequency response to the displacement amplitude of the diaphragm exhibits a peak in phase with the diaphragm resonant frequency f = 500 Hz. The maximum synthetic jet velocity for each configuration is in accordance with the diaphragm resonant frequency f[14].

1.3 Computational cases

In simulation, air is viewed as fluid medium. Let $t^*=t/T–N$ be dimensionless time, T is vibration period of the PZT-diaphragm, and N is number of the vibration period.

The primary jet mass rate and momentum on the conduit exit are given by

$$\begin{aligned} \dot{m}_p &= \rho H U_{ave} \\ M_p &= \rho H U_{ave}^2 \end{aligned} \tag{3}$$

The sums of mass rate ratio and momentum ratio between the synthetic jet flow and the primary jet flow per unit blowing span of the actuator are

$$\begin{aligned} r_{mi} &= \int_0^{T/2} \dot{m}_i \mathrm{d}t \Big/ \int_0^{T/2} \dot{m}_p \mathrm{d}t \\ r_{MPi} &= \int_0^{T/2} M_i \mathrm{d}t \Big/ \int_0^{T/2} M_p \mathrm{d}t \end{aligned} \tag{4}$$

For brevity, three primary jet velocities are chosen for discussion, i.e., U_{ave} = 20.0 m/s, 10.0 m/s, and 7.5 m/s, to which correspond the characteristic frequencies of the primary jet $f_c = U_{ave}/H$ = 1 000 Hz, 500 Hz, and 375 Hz, and the conduit Reynolds numbers $Re_H = U_{ave}H/\nu$ = 27 300, 13 700, and 10 300, where ν is the kinematic viscosity. Then three baseline cases of the SB in the middle of two exits (Case 6, 10, 14, shown in Table 1), three cases of the SB down by 0.5 mm (Case 7, 11, 15), three cases of the SB up by 0.5 mm (Case 8, 12, 16), and three cases of jet vectoring by traditional SJA (Case 5, 9, 13) are simulated and discussed. The parameters r_m, r_{MPi} and r_f ($r_f = f / f_c$) are calculated from Eqs.(3) and (4). The computational cases and parameters of vectoring primary jet using SJAs are summarized in Table 1.

1.4 Grids and boundary conditions

In the baseline cases (6, 10, and 14), the computational domain and grid distribution are illustrated in Table 2. In Case 7, 11, and 15, the down exit nozzle domain is 0.5 mm × 4 mm and its computational grids are 5 × 40, and the up exit nozzle domain is 1.5 mm × 4 mm and its computational grids are 15 × 40. In Case 8, 12, and 16, the down exit nozzle domain is 1.5 mm × 4 mm and its computational grids are 15 × 40, and the up exit nozzle domain is 0.5 mm × 4 mm and its computational grids are 5 × 40. In Case 5, 9, and 13, the exit nozzle domain of the traditional SJA is 1 mm × 4 mm and the grids are 10 × 40.

An inflow boundary along the actuator membrane is defined by Eq.(2). A velocity inlet condition

is adopted along the primary jet inlet boundary. Outflow conditions are specified along the free boundaries, and no-slide wall conditions are applied along the solid walls.

1.5 Validations

Numerical simulations and PIV experiments of a novel SJA in quiescent air are compared in the work[14]. With reliable computing results, Fig.3 shows the comparison between the PIV experiment and the numerical simulation. The experiment of jet vectoring by synthetic jets under the similar conditions was described in the literature[5], and the numerical simulation of flow field depicted in the study[14]. Fig.4 compares the experiment with the numerical simulation. The vectoring angle in the numerical simulation shown in Fig.4(b) is of the same order as in the experiment shown in Fig.4(a). The numerical accuracy proves to be acceptable.

Table 1 Computational cases and parameters of vectoring primary jet using SJAs

	SJA		Primary Jet		Parameters			
Case	Traditional-	Novel-	Velocity/m·s^{-1}		r_{mi} (r_{m1} , r_{m2})		r_{MPi}	(r_{MP1}, r_{MP2})
1	1	0	0	--	--		--	
2	0	1, middle	0	--	--		--	
3	0	1, down	0	--	--		--	
4	0	1, up	0	--	--		--	
5	1	0	20.0	0.40	0.028		0.022	
6	0	1, middle	20.0	0.40	0.028	0.028	0.022	0.022
7	0	1, down	20.0	0.40	0.028	0.028	0.075	0.010
8	0	1, up	20.0	0.40	0.028	0.028	0.010	0.075
9	1	0	10.0	0.80	0.056		0.086	
10	0	1, middle	10.0	0.80	0.056	0.056	0.086	0.086
11	0	1, down	10.0	0.80	0.056	0.056	0.300	0.040
12	0	1, up	10.0	0.80	0.056	0.056	0.040	0.30
13	1	0	7.5	1.07	0.075		0.150	
14	0	1, middle	7.5	1.07	0.075	0.075	0.150	0.150
15	0	1, down	7.5	1.07	0.075	0.075	0.530	0.071
16	0	1, up	7.5	1.07	0.075	0.075	0.071	0.530

Note: 1-forced, 0-unforced; middle-SB in the middle, down-SB shifts down 0.5 mm, up-SB shifts up 0.5 mm.

Table 2 Computational domain and grid distribution for baseline case (Case 6, 10, 14)

Designation	Domain (x×y)/mm	Grid (x×y)	Remarks
Primary Jet Conduit	100×20	100×50	Dense to exit and wall
SJA Cavity	46×4	80×40	Divided evenly in y-direction, dense to exit
SJA Exit Nozzle	4×1	40×10	Divided evenly
External Surroundings	300×300	200×250	Dense in center and to wall

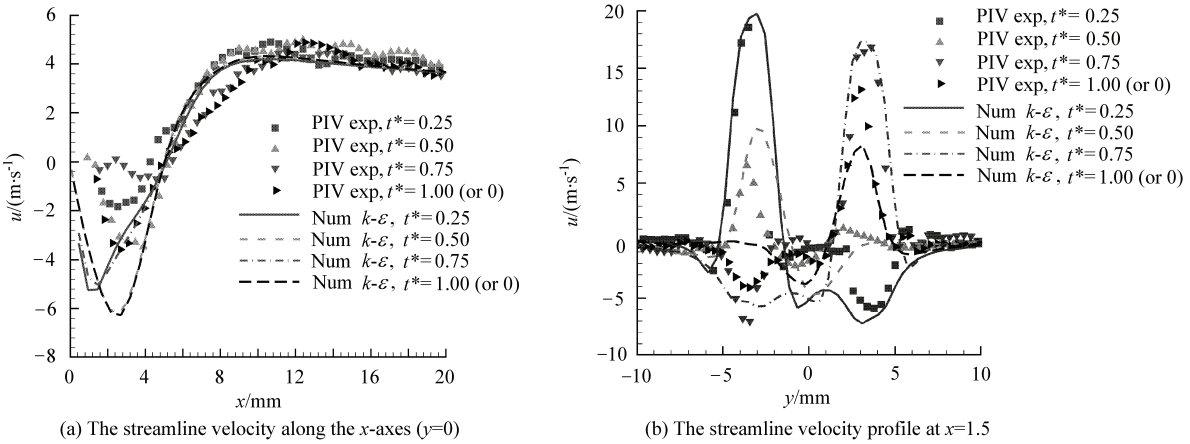

(a) The streamline velocity along the x-axes (y=0) (b) The streamline velocity profile at x=1.5

Fig.3 Comparison between PIV experiment and simulation for the novel SJA[14].

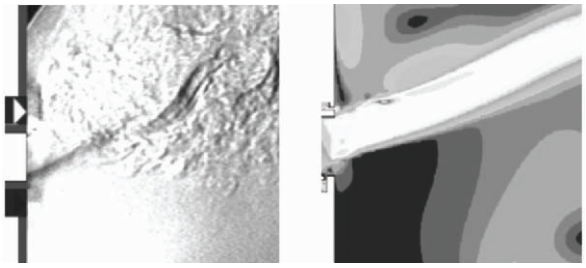

(a) Experiment[5] (b) Simulation[14]

Fig.4 Comparison between experiment and simulation for jet vectoring.

2 Results and Analysis

Figs.5-7 separately show the velocity magnitude and vorticity near the exit of the jets and the primary jet velocities U_{ave}= 20.0 m/s, 10.0 m/s, and 7.5 m/s, when t^* = 0.5.

The vectoring angle of the primary downstream ϕ can be determined by following equation[8]:

$$\phi = \tan^{-1}\left(\frac{y_- + y_+}{2x}\right) \tag{4}$$

where $y_+ > y_-$, y_- and y_+ are the y-coordinate of the points of primary jet velocty $u = 0.5u_{max}$ with u_{max} being the maximum flow velocity of the primary jet. Table 3 lists the results of the vectoring angle of the primary downstream at x = 40 mm = 2H for Cases 5-16.

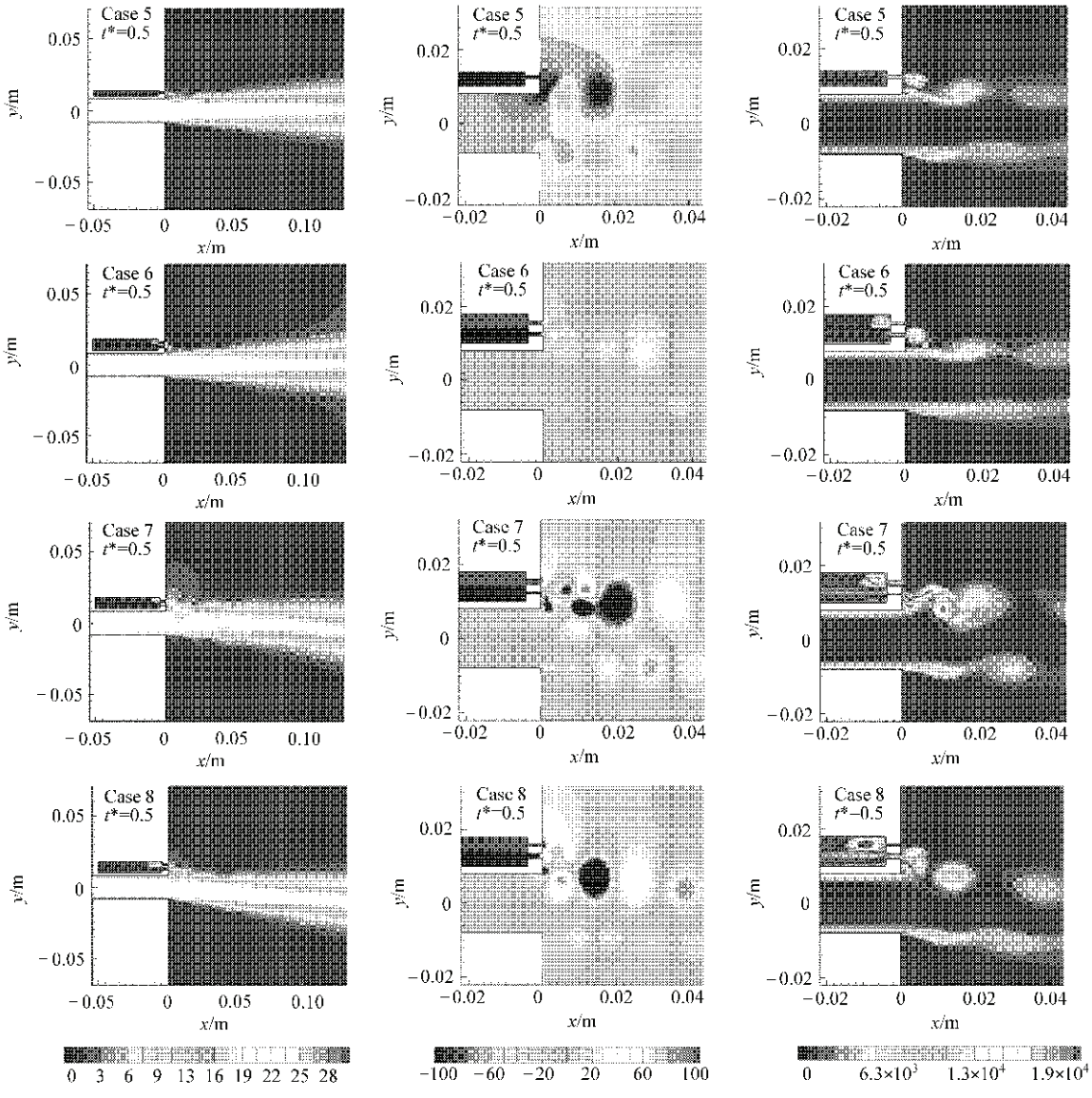

(a) Velocity (b) Static pressure (c) Vorticity

Fig.5 Velocity magnitude, static pressure and vorticity near the exit of the jets (U_{ave} = 20.0 m/s).

Table 3 Vectoring angle ϕ of the primary downstream x = 40 mm

Case	ϕ(°)	Function of SJA
5	0	None
6	0	None
7	–3	Push
8	–9	Push
9	3	Pull
10	0	None
11	8	Pull
12	–18	Push
13	5	Pull
14	1	Pull
15	11	Pull
16	–24	Push

In the former work[8], it was concluded that the lower pressure, the momentume impulse, and the entrainment of the primary jet flow by the synthetic jet flow are the main factors that govern the primary jet vectoring angles.

In a given traditional SJA, the fixed flow direction of the synthetic jet determines the momentum of a synthetic jet whether to resist or to induce the vectoring of the primary jet[7]. As a result, the existing synthetic actuator is capable of performing only one of the functions "pull" and "push" in vectoring a primary jet as with the Case 9 and Case 13 in Fig.6(a) and Fig.7(a). In Fig.6(b) and Fig.7(b), the lower pressure regions between the synthetic jets and the primary jets in Cases 5, 9 and 13, contribute to the vectoring forces and lead to an upward turn-

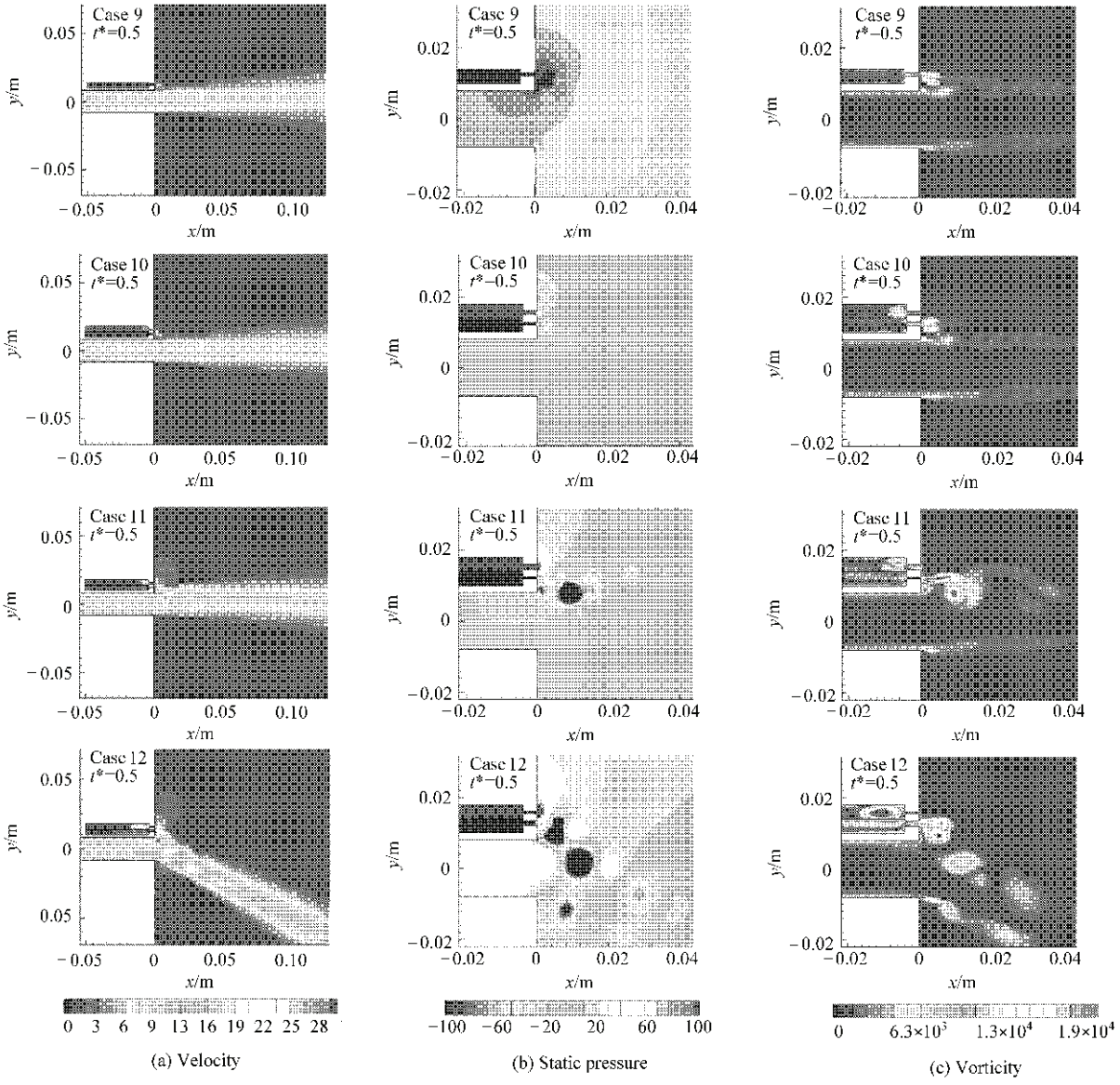

Fig.6 Velocity magnitude, static pressure and vorticity near the exit of the jets (U_{ave}=10.0 m/s).

ing of the primary jet at the conduit exit. In the nearby field, the primary jet fluid entrained by the synthetic jet diverts continuously. The vorticities of synthetic jets shown in Fig.5(c) and Fig.7(c) contribute to the entrainment. Therefore, the actuators in Case 9 and Case 13 fulfill a "pull" function.

However, in the novel SJA, things are different. With the SB inside it being shifted downward and the novel synthetic jet turned upward, the lower pressure region between the synthetic jets and the primary jets appears with its momentum induced to fulfill the function of pulling and turning the primary jet upward as with the Case 15 in Fig.7. On the other hand, with the SB shifted upward and the novel synthetic jet turned downward, the higher-pressure region between the synthetic jets and the primary jets occurs with its momentum to perform the function of pushing and turning the primary jet downward as with the Case 8 in Fig.5, Case 12 in Fig.6, and Case 16 in Fig.7.

When the SB is located in the middle, as in Case 6, Case 10, and Case 14, two fluid puffs out of phase with equal momentum will be forced out of the novel SJA, and the "self-support" between the two fluid puffs[14] makes it too weak to vector the primary jet.

It is also found that the novel synthetic jet must be strong enough to avoid the entrainment of the

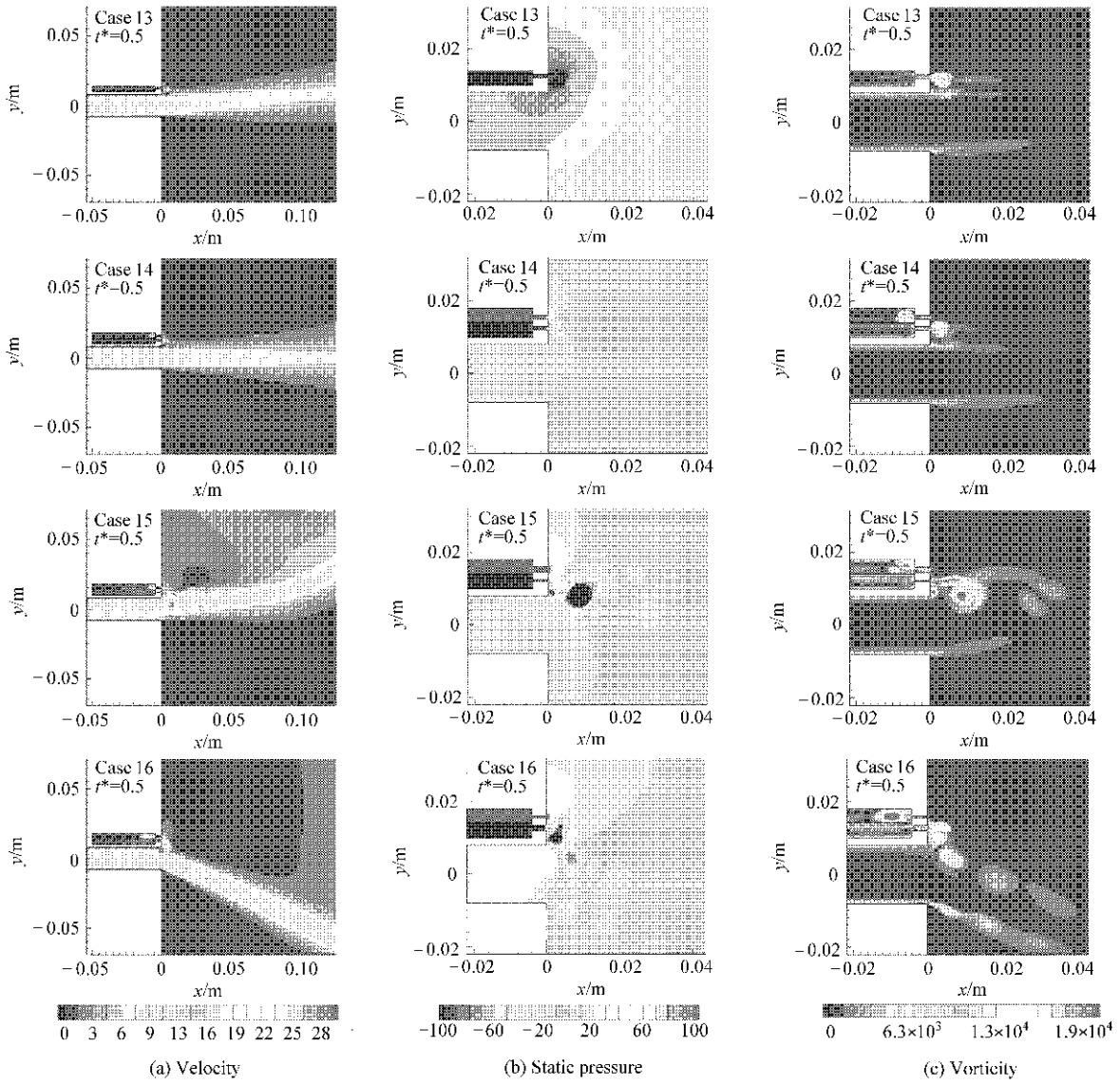

Fig.7 Velocity magnitude, static pressure and vorticity near the exit of the jets (U_{ave} = 7.5 m/s).

primary jet fluid, or prevent its flow from being vectored by the primary jet in the opposite direction. For example, in Case 7 in Fig.5, the novel synthetic jet is vectored downward by the primary jet flow causing its momentum to resist the vectoring of the primary jet and to push the primary jet turning downward.

As shown in Table 3, for a given set of primary jet and the synthetic jet controlled by the actuators, the vectoring angles of a primary jet may be different. In general, the novel SJA is more efficient than the existing traditional one to vector the primary jet, which is ascribed to their parameters matching the primay jet being different, especially the momentum ratio r_{MPi}. The results in Table 3 also show that, the down-vectoring angle of a primary jet pushed by a novel SJA (Case 12 and Case 16) is greater than its up-vectoring angle pulled by the same actuator (Case 11 and Case 15). The reason lies in the use of the Coanda effect made by the actuator when performing the "push" function, which means that as the novel synthetic jet turns downward, it attaches the down wall and almost directly pushes the primary jet downward.

3 Conclusions

A novel SJA to vector a primary jet is introduced. The characteristic feature of the actuator is the shifting of a SB inside it to govern its work. When the SB moves downward, the actuator pulls the primary jet upward. And conversely, the upward movement of the SB makes the actuator push the primary jet downward. Consequently, one single novel SJA has the ability to fulfill both "push" and "pull" functions to vector the primary jet that a traditional SJA does not have. This implies that the novel SJA possesses the potentiality to replace the existing one in a variety of flow control systems including those that the existing one has failed to meet their requirements.

In general, the novel SJA vectoring the primary jet is proved to be more efficient than the traditional one. Moreover, in a novel actuator, its "push" function is superior to its "pull" function in terms of efficiency.

More work is required to popularize novel SJAs into new realms. This includes a deeper study on the jet vectoring control by means of a novel SJA.

Acknowledgements

The authors gratefully acknowledge the financial support from the National Nature Science Foundation of China (Grants: 50176055 and 90205016). Thanks are also expressed to Professor Liu and Dr Huang for their contribution to this paper.

References

[1] Kral L D. Active flow control technology. ASME Paper No.FEDSM2001-18196, 2001.

[2] Glezer A, Amitay M. Synthetic jets. Ann Rev Fluid Mech 2002; 34: 503-529.

[3] Li Y, Ming X. Control of two-dimensional jets using miniature zero mass flux jets. Chinese Journal of Aeronautics 2000; 13(3): 129-133.

[4] Zhao H, Yang Z G, Lou H J. Experimental investigation of flow characteristics of synthetic jet and its preliminary application to combustion. Journal of Aerospace Power 2004; 19(5): 512-519. [in Chinese]

[5] Smith B L, Glezer A. Vectoring and small-scale motions affected in free shear flows using synthetic jet actuators. AIAA Paper 97-0213, 1997.

[6] Smith B L, Glezer A. Jet vectoring using synthetic jets. J Fluid Mech 2002; 458: 1-34.

[7] Guo D H, Cary A. Numerical simulation of vectoring control of a primary jet with synthetic jet. AIAA J 2003; 41(12): 2364-2370.

[8] Luo Z B, Xia Z X. An optimal mode of jet vectoring using synthetic jet actuators. The 8th International Symposium on Fluid Control, Measurement and Visualization. Chengdu, China, 2005.

[9] Luo Z B, Xia Z X, Liu B. A synthetic jet actuator with a diaphragm, two cavities and two slots. Chinese Patent, No: 200610031334.0. [in Chinese]

[10] Luo Z B, Xia Z X, Liu B. New generation of synthetic jet actuators. AIAA J 2006; 44(10): 2418-2420.

[11] Luo Z B, Xia Z X, Liu B. An adjustable synthetic jet by a novel PZT-driven actuator. Journal of Physics: Conference Series 2006;

34: 487-492.

[12] Luo Z B, Xia Z X. Numerical simulation of synthetic jet flow field and parameter analysis of actuator. Journal of Propulsion Technology 2004; 25: 199-205.

[13] Luo Z B, Xia Z X. A novel valve-less synthetic jet-based micro-pump. Sensors and Actuators A 2005; 122(1): 131-140.

[14] Luo Z B. Principle of synthetic jet and dual synthetic jets, and their applications in jet vectoring and micro-pump. Ph.D. thesis, National University of Defense Technology, 2006. [in Chinese]

Biography:

LUO Zhen-bing Born in 1979, he received a M.S. degree and a Ph.D. from the National University of Defense Technology in 2002 and 2006 respectively. His academic interest is the synthetic jets and the active flow control technology.

E-mail: luozhenbing@163.com